

Article

Synthesis of Coumarin Derivatives: A New Class of Coumarin-Based G Protein-Coupled Receptor Activators and Inhibitors

Zhe Fu ¹, Linjie Zhang ¹, Sijin Hang ¹, Shiyi Wang ², Na Li ¹, Xiaojing Sun ¹, Zian Wang ¹, Ruilong Sheng ³ , Fang Wang ⁴, Wenhui Wu ¹  and Ruihua Guo ^{1,5,6,*} 

¹ College of Food Science and Technology, Shanghai Ocean University, Shanghai 201306, China; fzshou2019@163.com (Z.F.); ljzhang20010428@163.com (L.Z.); sjhang2022@163.com (S.H.); ln16658@163.com (N.L.); sunxj1997@163.com (X.S.); wzamengnan1999@163.com (Z.W.); whwu@shou.edu.cn (W.W.)

² AIEN Institute, Shanghai Ocean University, Shanghai 201306, China; wjcx3111@163.com

³ CQM—Centro de Química da Madeira, Campus da Penteada, Universidade da Madeira, 9000-390 Funchal, Portugal; ruilong.sheng@staff.uma.pt

⁴ School Basic Medicine, Shanghai University of Medicine and Health Science, Shanghai 201318, China; wangf_18@sumhs.edu.cn

⁵ Laboratory of Quality and Safety Risk Assessment for Aquatic Product on Storage and Preservation, Ministry of Agriculture, Shanghai 201306, China

⁶ Engineering Research Center of Aquatic-Product Processing & Preservation, Shanghai 201306, China

* Correspondence: rhguo@shou.edu.cn



Citation: Fu, Z.; Zhang, L.; Hang, S.; Wang, S.; Li, N.; Sun, X.; Wang, Z.; Sheng, R.; Wang, F.; Wu, W.; et al. Synthesis of Coumarin Derivatives: A New Class of Coumarin-Based G Protein-Coupled Receptor Activators and Inhibitors. *Polymers* **2022**, *14*, 2021. <https://doi.org/10.3390/polym14102021>

Academic Editor: Prashanth Asuri

Received: 14 March 2022

Accepted: 4 May 2022

Published: 15 May 2022

Publisher's Note: MDPI stays neutral with regard to jurisdictional claims in published maps and institutional affiliations.



Copyright: © 2022 by the authors. Licensee MDPI, Basel, Switzerland. This article is an open access article distributed under the terms and conditions of the Creative Commons Attribution (CC BY) license (<https://creativecommons.org/licenses/by/4.0/>).

Abstract: To expand the range of daphnetin-based inhibitors/activators used for targeting G protein-coupled receptors (GPCRs) in disease treatment, twenty-five coumarin derivatives 1–25, including 7,8-dihydroxycoumarin and 7-hydroxycoumarin derivatives with various substitution patterns/groups at C3-/4- positions, were synthesized via mild Pechmann condensation and hydroxyl modification. The structures were characterized by ¹H NMR, ¹³C NMR and ESI-MS. Their inhibition or activation activities relative to GPCRs were evaluated by double-antibody sandwich ELISA (DAS-ELISA) in vitro. The results showed that most of the coumarin derivatives possessed a moderate GPCR activation or inhibitory potency. Among them, derivatives 14, 17, 18, and 21 showed a remarkable GPCR activation potency, with EC₅₀ values of 0.03, 0.03, 0.03, and 0.02 nM, respectively. Meanwhile, derivatives 4, 7, and 23 had significant GPCR inhibitory potencies against GPCRs with IC₅₀ values of 0.15, 0.02, and 0.76 nM, respectively. Notably, the acylation of hydroxyl groups at the C-7 and C-8 positions of 7,8-dihydroxycoumarin skeleton or the etherification of the hydroxyl group at the C-7 position of the 7-hydroxycoumarin skeleton could successfully change GPCRs activators into inhibitors. This work demonstrated a simple and efficient approach to developing coumarin derivatives as remarkable GPCRs activators and inhibitors via molecular diversity-based synthesis.

Keywords: coumarin; G protein-coupled receptors; synthesis; structure–activity relationships

1. Introduction

G protein-coupled receptors (GPCRs) are a large family of membrane-protein receptors with a transmembrane α -helix structure which are involved in a variety of physiological functions and have a variety of complex and key signaling pathways for bioactivities [1,2]. The most used classification of GPCRs divides them into six categories: rhodopsin-like receptors (class A), secretin-like receptors (class B), metabotropic glutamate receptors (class C), pheromone receptors (class D), cAMP receptors (class E), and frizzled/smoothed family receptors (class F). Among them, class A is the most studied, and the structures of these receptors have also been identified. However, few studies on the structures of protein receptors have been reported for class B-F. In 2013, the first human glucagon-receptor structure

of class B GPCRs was confirmed [3]. The GPCRs' relevant activities are regulated by two signaling pathways: cAMP signaling and phosphatidylinositol signaling [4]. More than 30% of the drugs approved by the FDA are able to target GPCRs [5]. For instance (Figure 1), Naloxegol is used for opioid-induced constipation (a μ -opioid receptor antagonist) [6], Droxidopa is used for symptomatic postural hypotension [7], Aripiprazole Lauroxil is used for schizophrenia (a dopamine D2 receptor, and a partial agonist of the 5-HT_{1A} receptor and the 5-HT_{2A} receptor antagonist) [8], Brexpiprazole is used for depression (with mixed opioid receptor activity) [9], and Olodaterol is used for chronic obstructive pulmonary disease (a β 2-adrenergic receptor agonist) [10]. Many GPCRs-targeting drugs still have complicated chemical structures or tedious synthesis routes, which increase their costs in large-scale production. Therefore, it is necessary to develop simple-structured, easy-to-synthesize, and new GPCR-targeting drugs/compounds for disease treatment.

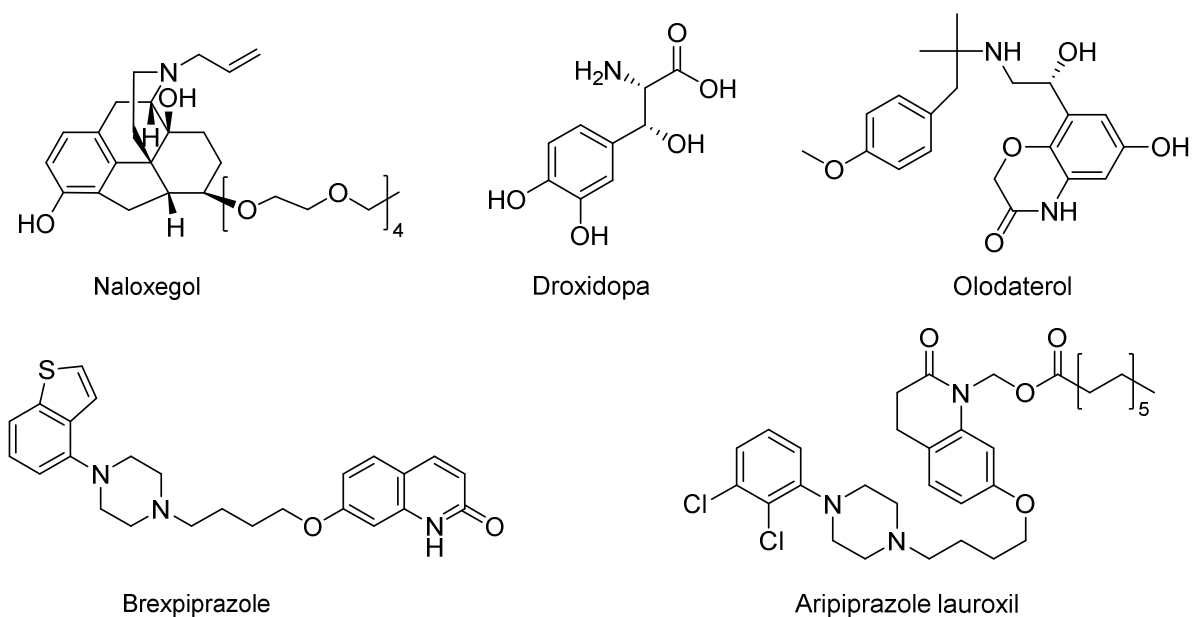


Figure 1. Chemical structures of drugs targeting GPCRs approved by the FDA.

Natural products with various skeletons and diverse bioactivities are considered important sources for drug discovery [11–25]. Since the discovery of natural coumarin in 1820 [26], numerous coumarin derivatives have been extracted from the secondary metabolites of many plant species [27]. Coumarin derivatives exhibit diverse bioactivities, such as anti-bacterial [28,29], anticoagulant [30], anti-inflammatory [31,32], anti-tumor [33–35], and antioxidant effects [36], etc. [37–42]. Thus, they have received a large amount of attention from synthetic chemists. Up until now, some synthetic methodologies, including the Pechmann condensation [43], the Perkin reaction [44], Knoevenagel condensation [45], metal-catalyzed cyclization [46], the Wittig reaction [47], and other reactions [48,49], have been developed to prepare coumarin derivatives. Previously, we reported that daphnetin (a naturally occurring coumarin) derivatives (Figure 2) with various substitution patterns/groups exhibited activities from inhibitory potency to activation potency in GPCRs. The optimized compound 4a and its derivatives showed the highest inhibitory or activation potency in GPCRs [50,51].

In order to further improve the activities of coumarin derivatives by expanding their molecular diversity, 7, 8-dihydroxycoumarin and 7-hydroxycoumarin derivatives with various substitution patterns/groups at the C-3/-4 positions were synthesized and characterized in this study. Their pharmaceutical potency in GPCRs were evaluated by a double-antibody sandwich ELISA (DAS-ELISA) *in vitro*. The synthesized compounds were used as an antigen in the kit. The enzyme substrate and the specific antibody in the enzyme plate formed a 'sandwich'. Finally, the substrate of the enzyme was added,

and the content of antigen was determined based on the absorbance of the enzymolysis product. Detailed steps are shown in “2.4 DAS-ELISA evaluation of coumarin derivatives on GPCRs”. It was disclosed that derivatives 14, 17, 18, and 21 displayed a remarkable activation potency in GPCRs with EC_{50} values of 0.03, 0.03, 0.03, and 0.02 nM, respectively. On the other hand, derivatives 4, 7, and 23 possessed significant inhibitory potency on GPCRs with IC_{50} values of 0.15, 0.02, and 0.76 nM, respectively.

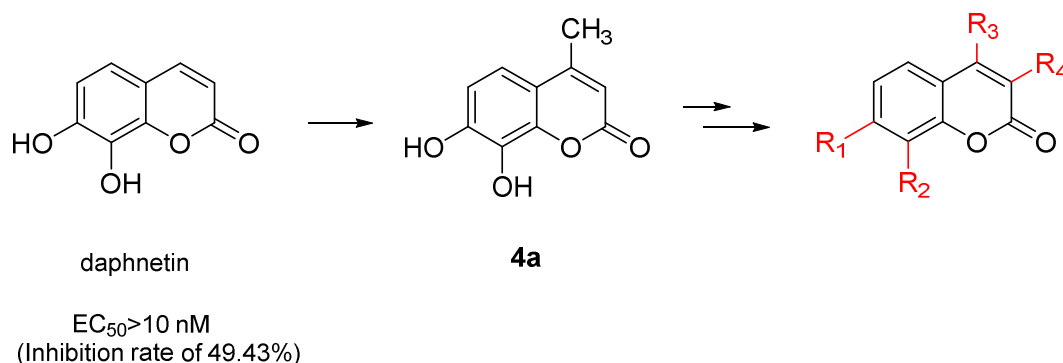


Figure 2. Chemical structures of daphnetin and its derivatives for the development of GPCR inhibitors/activators.

2. Materials and Methods

2.1. Materials and Methods

All chemicals and reagents used in the study were commercially available and used as received. Thin-layer chromatography (TLC) and column chromatography (300–400 mesh) were achieved using instruments from Qingdao Makall Group Co., Ltd. (Qingdao, China). ^1H NMR and ^{13}C NMR spectra were recorded on a Bruker DRX-500 ($^1\text{H}/^{13}\text{C}$, 500 MHz/125 MHz) spectrometer (Bruker, Bremerhaven, Germany) or a JEOL 400YH ($^1\text{H}/^{13}\text{C}$, 400 MHz/100 MHz) and chemical shifts were given in δ with the TMS as an internal reference. The ESI-MS spectroscopy was measured on an Advantage Max LCQ Thermo-Finnigan mass spectrometer. The ELISA kit was purchased from Shanghai Fusheng Industry Co., Ltd. (Shanghai, China), and the standard in the kit was Class B GPCRs.

2.2. General Procedure for Preparation the Derivatives 1–25

2.2.1. General Procedure for Preparation of Derivatives 1–6

Pyrogallol (1.0 equiv.) and scandium (III) trifluoromethanesulfonate ($\text{Sc}(\text{OTf})_3$) (0.1 equiv.) were added to a solution of appropriately different β -ketoesters (1.0 equiv.) at room temperature. The reaction mixture was stirred at 85 °C until the starting material disappeared on the TLC. The reaction mixture was quenched with 50 mL of water and extracted with CH_2Cl_2 (3×50 mL). The combined organic layer was washed three times with 50 mL of brine, dried over anhydrous Na_2SO_4 , concentrated under reduced pressure, and then purified by a column chromatography on the silica gel to obtain derivatives 1–6 [52–54]. Finally, the molecular structures of the synthesized derivatives were fully characterized in the Supplementary Materials (Figures S1–S18).

2.2.2. General Procedure for Preparation of Derivatives 7 and 8

To a solution of derivative 6 (1 equiv.) in pyridine (1.0 mL), DMAP (0.5 equiv.) and Acetic anhydride or propionic anhydride (4.0 equiv.) were added in and stirred at room temperature until the starting material disappeared on the TLC. Then, the reaction mixture was diluted with 50 mL of CH_2Cl_2 and washed three times with 50 mL of 5% HCl and saturated NaHCO_3 (3×30 mL). After that, the organic layer was dried over anhydrous Na_2SO_4 and then concentrated under reduced pressure. The residue was purified by a column chromatography on the silica gel to access derivatives 7 [55] and 8. Finally,

the molecular structures of the synthesized derivatives were fully characterized in the Supplementary Materials (Figures S19–S24).

2.2.3. General Procedure for Preparation of Derivatives 9–20

Resorcinol (1.2 equiv.) and scandium (III) trifluoromethanesulfonate ($\text{Sc}(\text{OTf})_3$) (0.1 equiv.) were added to a solution of appropriately different β -ketoesters (1.0 equiv.) at room temperature. The reaction mixture was stirred at 85 °C until the starting material disappeared on the TLC. The reaction mixture was quenched with 50 mL of water and extracted with CH_2Cl_2 (3×50 mL). The combined organic layer was washed three times with 50 mL of brine, dried over anhydrous Na_2SO_4 , concentrated under reduced pressure, and then purified by a column chromatography on the silica gel to obtain derivatives 9–20 [52,56–59]. Finally, the molecular structures of the synthesized derivatives were fully characterized in the Supplementary Materials (Figures S25–S57).

2.2.4. General Procedure for Preparation of Derivatives 21

Derivative 9 (100 mg, 1.0 equiv.) was dissolved in a solution of sodium hydroxide (16.4 mg, 10 equiv.) in water (0.41 mL) and the mixture was maintained at an ice bath temperature. A solution of 2, 4-dichloropyrimidine (122.1 mg, 2.0 equiv.) in acetone (1.6 mL) was added dropwise, and the mixture was stirred and refluxed until the starting material disappeared on the TLC [60]. The reaction mixture was quenched with 50 mL of water and extracted with CH_2Cl_2 (3×50 mL). The combined organic layer was washed three times with 50 mL of brine, dried over anhydrous Na_2SO_4 , concentrated under reduced pressure, then purified by a column chromatography on the silica gel to obtain derivatives 21. Finally, the molecular structures of the synthesized derivatives were fully characterized in the Supplementary Materials (Figures S58–S61).

2.2.5. General Procedure for Preparation of Derivatives 22 and 23

To a solution of derivatives 17 (1 equiv.) in acetone (2.0 mL), K_2CO_3 (10 equiv.) was added at room temperature. After half an hour, iodide methane or bromoethane (3.0 equiv.) was added and the resulting mixture was stirred at 65 °C until the starting material disappeared from the TLC. The residue was added with 50 mL water, and the following mixture solution was extracted with CH_2Cl_2 (3×50 mL). The combined organic layers were washed with brine, and then dried over anhydrous Na_2SO_4 . After the removal of the solvent under reduced pressure, the crude products were produced; these were purified by column chromatography on silica gel to achieve derivatives 22 [61] and 23. Finally, the molecular structures of the synthesized derivatives were fully characterized in the Supplementary Materials (Figures S61–S66).

2.2.6. General Procedure for Preparation of Derivatives 24 and 25

A solution of derivative 7 (1 equiv.), DMAP (0.5 equiv.) and acetic anhydride or propionic anhydride (4.0 equiv.) in pyridine (1.0 mL) was stirred at room temperature until the starting material disappeared on the TLC. Then the reaction mixture was diluted with 50 mL of CH_2Cl_2 and washed three times with 50 mL of 5% HCl and saturated NaHCO_3 (3×30 mL). Following, the organic layer was dried over anhydrous Na_2SO_4 and then concentrated under reduced pressure. The residue was purified by a column chromatography on the silica gel to access derivatives 24 and 25. Finally, the molecular structures of the synthesized derivatives were fully characterized in the Supplementary Materials (Figures S67–S72).

2.3. Sample Pretreatment

All the synthesized coumarin derivatives were dissolved in 500 μL of DMSO, and then diluted to 1 mL by distilled water to get 1 mg/mL of stock solution. Finally, the stock solution was diluted to 1000 $\mu\text{g}/\text{L}$, 10 $\mu\text{g}/\text{L}$, 0.1 $\mu\text{g}/\text{L}$, and 0.001 $\mu\text{g}/\text{L}$ in turn and stored in a refrigerator at 4 °C for reserve.

2.4. DAS-ELISA Evaluation of Coumarin Derivatives on GPCRs

The inhibitory/activation activities of all of the synthesized coumarin derivatives on GPCRs were evaluated through incubation using mouse GPCRs provided by the ELISA kit (Shanghai Fusheng Industrial Co., Ltd. Shanghai, China). Other components of the kit included a water solution (30 times concentrated), a HRP conjugation reagent, a sample diluent, a standard diluent, standard, a chromogenic reagent A, a chromogenic reagent B, and a stop solution.

The 15 μL of stock solution and 15 μL of diluted standard solution were thoroughly mixed and incubated at 37 $^{\circ}\text{C}$ for 10 mins to prepare a reaction solution. The assay was conducted according to the kit protocol, that is, by adding the 25 μL of reaction solution to a 96-well enzyme-labeled plate containing solid phase anti-GPCRs antibodies. Then the plate was incubated for 30 mins at 37 $^{\circ}\text{C}$. Then, 25 μL of Chromogener A and 25 μL of Chromogener B were then added to react. Finally, 25 μL of the termination solution was added to each well to terminate the reaction and the mixture was fully mixed. Derivatives were tested in four different concentrations: 10 ng/L, 1 ng/L, 0.1 $\mu\text{g}/\text{mL}$, and 10 $\mu\text{g}/\text{L}$. A diluent was prepared, dissolved and diluted with the other components of the kit according to the instructions in the kit, and a termination solution was added to the reaction. Then, the OD value was obtained by a microplate reader in 15 mins. All the derivatives were set into two independent experimental groups, and the inhibition of GPCRs, which was expressed as a percentage, was based on these groups [50,62–64].

3. Results and Discussion

3.1. Results

Chemistry

7,8-dihydroxycoumarin derivatives (1–8) and 7-hydroxycoumarin derivatives (9–25) with various substitution patterns/groups at C3-/4- positions were synthesized via Pechmann condensation. First, 7,8-dihydroxycoumarin derivatives 1–6 with different substituents at the C-4 position were synthesized, by a react pyrogallol with different β -ketoesters in the presence of Scandium(III) triflate ($\text{Sc}(\text{OTf})_3$) as the catalyst, through a one-pot synthesis (Scheme 1) [65]. Derivative 6 reacted with acetic anhydride and propionic anhydride in the presence of 4-dimethylaminopyridine (DMAP) as the catalyst in pyridine to produce the derivatives 7 and 8, respectively.

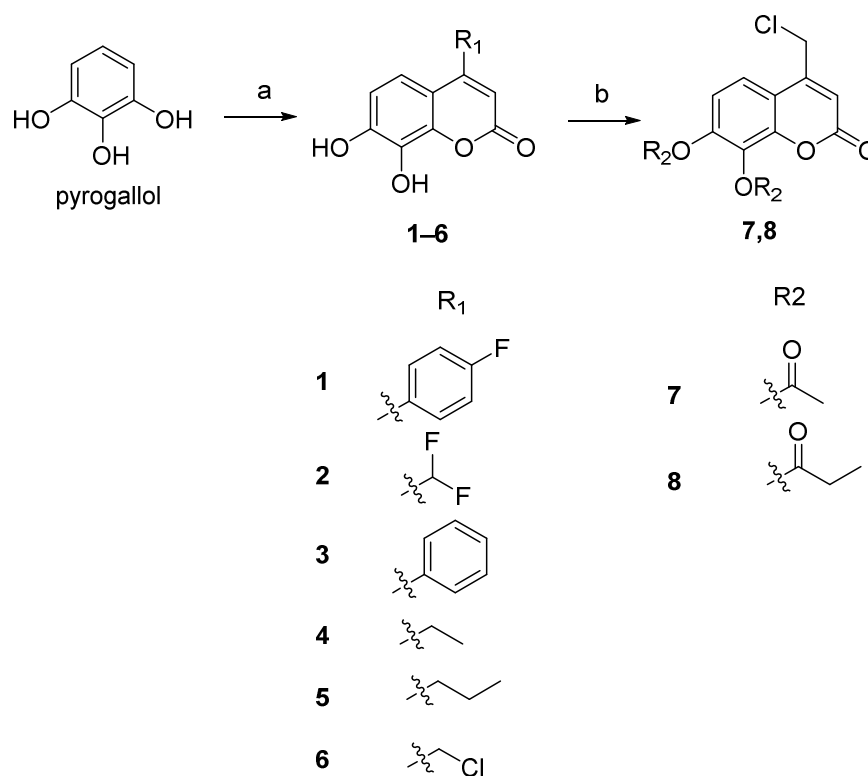
Similarly, resorcinol as the starting material, which reacts with different β -ketoesters in the presence of Scandium(III) triflate ($\text{Sc}(\text{OTf})_3$), was used to produce 7-hydroxycoumarin derivatives 9–25 with different substitution groups in C3-/C4- positions through a one-pot synthesis (Scheme 2). Then, derivative 9 reacted with 2,4-dichloropyrimidine in the presence of K_2CO_3 in acetone to afford derivatives 22 and 23. Derivative 15 reacted with acetic anhydride and propionic anhydride in the presence of DMAP to produce derivatives 24 and 25, respectively. Derivative 15 was treated with various CH_3I or $\text{C}_2\text{H}_5\text{Br}$ in the presence of K_2CO_3 in acetone or *N,N*-dimethylacetamide to achieve derivatives 22 and 23. All of the synthesized compounds were fully characterized by NMR and ESI-MS spectroscopy. All of the chemical shifts were expressed in parts per million (ppm) relative to internal tetramethylsilane (TMS), and coupling constants (J) were expressed in hertz (Hz). MS dates have been listed in the Supplementary Materials.

3.2. Discussion

Biological Evaluation of The Synthesized Coumarin Derivatives at GPCRs in Vitro

The as-synthesized twenty-five coumarin derivatives (1–25) were evaluated to determine their activities in GPCRs using the DAS-ELISA method [50,62]. The results showed that coumarin derivatives possessed different bioactivities in GPCRs ranging from inhibition to activation (Figure S73–S75). The GPCRs' inhibition/activation activity of each compound was expressed as the concentration of the compound that achieved a 50% inhibition (IC_{50})/50% activation (EC_{50}) effect of the GPCRs' standard at 10 ng/L. The results are shown in Table 1. Derivatives 1–25 had different activities on GPCRs, from inhibition

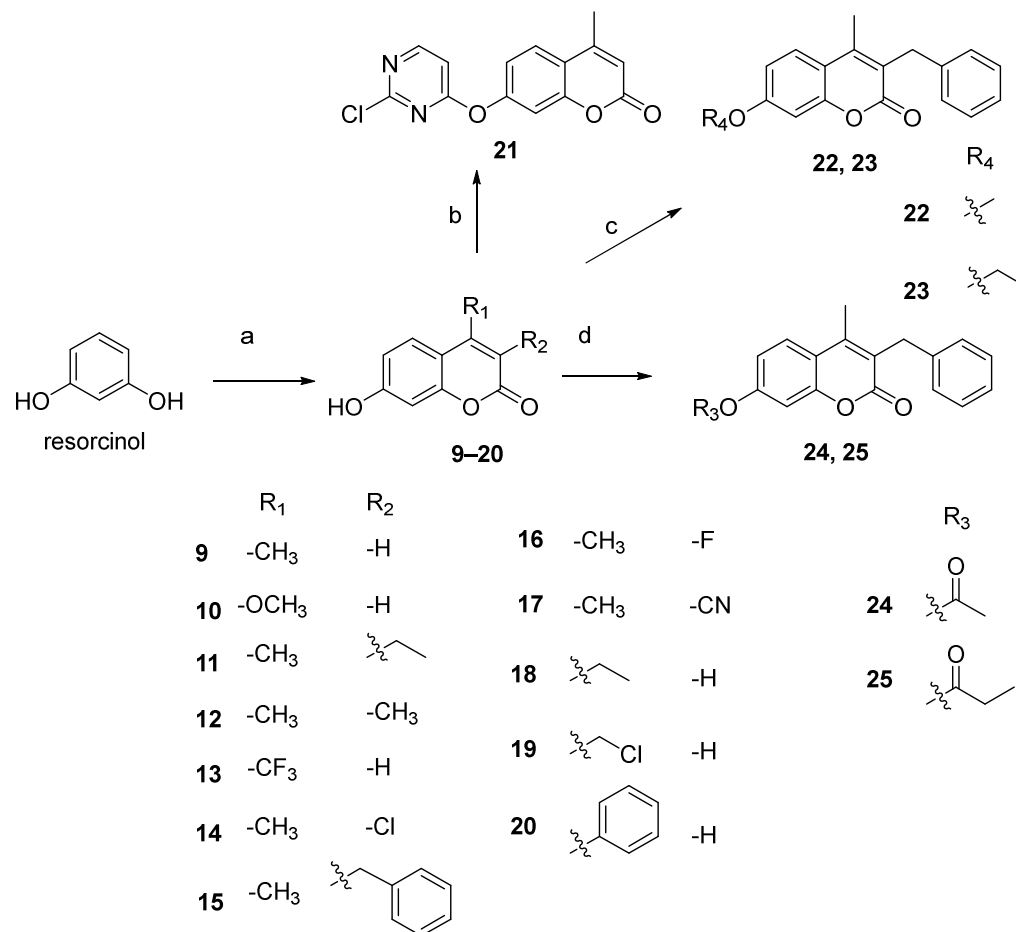
to activation. It can be seen that 7,8-dihydroxycoumarin derivatives 1 and 6 showed an activation potency on GPCRs with EC_{50} values of 0.56 and 0.49 nM, respectively, while derivatives 4, 5, 7, and 8 showed an inhibitory potency on GPCRs; among them, 4 and 7 exhibited a significant inhibitory potency, with IC_{50} values of 0.15 nM and 0.02, respectively. For 7-hydroxycoumarin derivatives 9, 11, 12, 14, 16–19, and 21 with different substitution patterns/groups at C-3 or C-4 positions possessed an activation potency on GPCRs with EC_{50} values in the range of 0.02–7.75 nM, while 13 and 15 had an inhibitory potency on GPCRs with IC_{50} values of 7.75 and 3.60 nM.



Scheme 1. Reagents and conditions: (a) $Sc(OTf)_3$, β -ketoesters, 80 °C, 0.5–2 h; (b) acetic anhydride or propionic anhydride, pyridine, DMAP, r.t., 2–3 h.

Daphnetin had a weak inhibitory activity in GPCRs with an inhibition rate of 49.43% at 10 ng/L. Previous work has demonstrated that the replacement of the methyl group at the C-4 position of daphnetin (4a) was beneficial for the activation potency on GPCRs [50]. Thus, it was expected that the introduction of 4-fluorophenyl, difluoromethyl, phenyl, ethyl, *n*-propyl, and chloromethyl groups to C-4 positions in daphnetin to derivatives 1–6 may lead to different activation activities in GPCRs. The result showed that 4-fluorophenyl derivatives 1 possessed a higher GPCR activation potency (EC_{50} = 0.56 nM) than that of derivative 4a (EC_{50} = 2.65 nM). However, the difluoromethyl derivative 2 and the phenyl derivative 3 had very low GPCRs-activation potencies, with EC_{50} > 39.37 nM and EC_{50} > 43.83 nM, respectively. Compared to derivative 4a, derivatives 4 and 5 with an alkylation of the hydroxyl group at C-4 positions completely lost their GPCRs-activation potency but retained their GPCRs-inhibition potency. Moreover, a decreasing inhibitory potency from 4 (IC_{50} = 0.15 nM) to 5 (IC_{50} = 3.77 nM) was observed with a lengthened side-chain. The C-4-chloromethyl derivative 6 showed a better activation potency on GPCRs with an EC_{50} of 0.49 nM than derivative 4a, indicating that the chloride substitution group at the C-4 methyl position possessed a remarkable GPCR activation potency. To further enhance the activation potency, derivatives 7 and 8 were designed and synthesized by introducing acetyl and propionyl groups at the C-7 and C-8 positions of derivative 6, and their activities in GPCRs were tested. Interestingly, derivatives 7 and 8 had no GPCR activation potency. Acetylated derivative 7 showed a remarkable inhibitory activity, with an

IC₅₀ of 0.02 nM. Meanwhile, the propionylated derivative 8 showed a moderate inhibitory activity, with an IC₅₀ of 6.86 nM. It can be disclosed that the acylation of hydroxyl groups at the C-7 and C-8 positions can successfully change GPCR activators into inhibitors.



Scheme 2. Reagents and conditions: (a) SC(OTf)₃, β -ketoesters, 80 °C, 0.5–2 h; (b) 2,4-dichloropyrimidine, acetone, NaOH, reflux 5 h; (c) CH₃I or CH₂CH₃Br, acetone, K₂CO₃, reflux 2–3 h; (d) acetic anhydride or propionic anhydride, pyridine, DMAP, r.t., 2–3 h.

To further investigate the structure–activity relationships (SARs), 7-hydroxycoumarin derivatives 9–25 with different substitution patterns/groups in C-4 were obtained by the reaction of resorcinol with different β -ketoesters. Derivatives 9, 18, and 19 with a methyl, ethyl, and chloromethyl group at the C-4 position had no GPCRs-inhibitory activity and showed a GPCRs- activation potency with EC₅₀ values of 1.25, 0.03, and 4.22 nM, respectively. Derivatives 10 and 13 possessed relatively weak inhibitory activities on GPCRs with IC₅₀ values of >48.84 and 7.75 nM, respectively. Furthermore, derivatives with methyl at the C-4 position were substituted by the different groups, C₂H₅, CH₃, Cl, benzyl, F, and CN at the C-3 position to produce derivatives 11, 12, and 14–17. Derivatives 11, 12, 14, 16–17 showed a high GPCRs-activation potency with EC₅₀ values in the range of 0.03–1.28 nM. However, derivative 15 with benzyl at the C-3 position possessed inhibitory activities against GPCRs from activation to inhibition with an EC₅₀ value of 3.60 nM, in comparison to derivative 9 (EC₅₀ = 1.25 nM) with CH₃ at C-3, suggesting that the benzyl group at the C-3 position was not suitable for activation potency among the investigated derivatives. Derivative 11 with C₂H₅ at C-3 (EC₅₀ = 1.28 nM) and derivative 12 with CH₃ at C-3 (EC₅₀ = 1.07 nM) retained their activation potencies on GPCRs compared to 9. The introduction of electron-withdrawing (Cl-, F- and CN-) groups to the C-3 position of derivative 9 produced derivative 14 (EC₅₀ = 0.03 nM), 16 (EC₅₀ = 0.24 nM), and 17 (EC₅₀ = 0.03 nM),

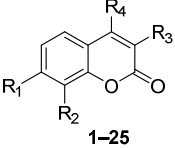
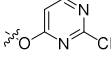
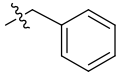
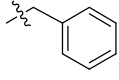
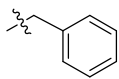
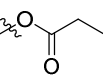
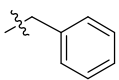
which seemed to increase the activation activity compared to derivative 9. These results indicated that electron-withdrawing groups at the C-3 position including Cl-, F- and CN-groups were more suitable for enhancing GPCRs-activation activities among the investigated derivatives.

Table 1. In vitro GPCR inhibition IC₅₀ or activation EC₅₀ (nM) activities of daphnetin and derivatives 1–25.

1–25

No.	R ₁	R ₂	R ₃	R ₄	EC ₅₀ (nM) (% Activation)	IC ₅₀ (nM) (% INHIBITION)
Daphnetin	-OH	-OH	-H	-H		>10 (49.43%)
1	-OH	-OH	-H		0.56 ± 0.02	-
2	-OH	-OH	-H		>43.83 (39.82%)	-
3	-OH	-OH	-H		>39.37 (35.75%)	-
4a	-OH	-OH	-H	-CH ₃	2.65 ± 0.25	-
4	-OH	-OH	-H		-	0.15 ± 0.01
5	-OH	-OH	-H		-	3.77 ± 0.58
6	-OH	-OH	-H		0.49 ± 0.32	-
7			-H		-	0.02 ± 0.01
8			-H		-	6.86 ± 0.04
9	-OH	-H	-H	-CH ₃	1.25 ± 0.89	-
10	-OH	-H	-H	-OCH ₃	-	>48.54 (33.58%)
11	-OH	-H		-CH ₃	1.28 ± 1.07	-
12	-OH	-H	-CH ₃	-CH ₃	1.07 ± 0.33	-
13	-OH	-H	-H	-CF ₃	-	7.75 ± 7.23
14	-OH	-H	-Cl	-CH ₃	0.03 ± 0.02	-
15	-OH	-H		-CH ₃	3.60 ± 0.11	-
16	-OH	-H	-F	-CH ₃	0.24 ± 0.21	-
17	-OH	-H	-CN	-CH ₃	0.03 ± 0.02	-
18	-OH	-H	-H		0.03 ± 0.01	-
19	-OH	-H	-H		4.22 ± 3.49	-

Table 1. Cont.

 1–25						
No.	R ₁	R ₂	R ₃	R ₄	EC ₅₀ (nM) (% Activation)	IC ₅₀ (nM) (% INHIBITION)
20	–OH	–H	–H		>41.97 (34.41%)	–
21		H	H	–CH ₃	0.02 ± 0.01	–
22		–H		–CH ₃	–	9.67 ± 2.59
23		–H		–CH ₃	–	0.76 ± 0.70
24		–H		–CH ₃	>35.67 (32.82%)	–
25		–H		–CH ₃	11.98 ± 9.47	–

A 2,4-dichloropyrimidine reaction with derivative 9 (IC₅₀ = 1.25 nM) produced derivative 21, which enhanced the inhibitory potency on GPCRs with IC₅₀ of 0.02 nM. Derivatives 22 and 23, obtained through the etherification of the hydroxyl group at the C-7 position in 15 (GPCR activator, EC₅₀ = 3.60 nM), presented an inhibitory potency on GPCRs with IC₅₀ of 9.67 and 0.76 nM, respectively. This result suggests that the etherification of the hydroxyl group can successfully change GPCRs activators into inhibitors, which is identical with our previous reports [50]. The ethylated derivative 23 displayed better inhibitory activity on GPCRs with an IC₅₀ of 0.76 nM, than the methylated derivative 22 (IC₅₀ = 9.76 nM), meaning that lengthening the side-chain at the C-7 position of derivative 15 was not beneficial for inhibitory activity. Derivatives 24 (EC₅₀ > 35.67 nM) and 25 (EC₅₀ = 11.98 nM) with the acylation of the hydroxyl group at the C-7 positions of derivative 15 (EC₅₀ = 3.60 nM) showed a decreasing activation potency, suggesting that the acylation of the hydroxyl group at C-7 was not beneficial for activation activity.

Inhibition rate = [OD(positive) – OD(test compound)]/[OD(positive) – OD(blank)] * 100%.

IC₅₀/EC₅₀ were obtained from Modified Karber formula [66] as the following:

$$\lg \rho = X_m - I \left[P - \frac{(3 - P_m - P_n)}{4} \right]$$

ρ : Concentration of compounds; X_m : Maximum dose; I = (Minimum inhibition rate)/Adjacent dose.

P : Sum of inhibition rates; P_m : Maximum inhibition rate; P_n : Minimum inhibition rate.

All values are the mean of two independent experiments ± SD.

4. Conclusions

In this work, twenty-five coumarin derivatives were synthesized via pyrogallol or resorcinol with different β -ketoesters. All synthesized derivatives were characterized by

NMR and MS spectroscopies, and their bioactivities in GPCRs were evaluated *in vitro* using the DAS-ELISA method. Most derivatives possessed a moderate activation or inhibitory potency in GPCRs. Among them, derivatives 1, 6, 9, 11, 12, 14, 16–18, and 21 showed a remarkable GPCR activation potency, with EC_{50} values in the range of 0.03–1.28 nM. Derivatives 4, 7, and 23 had significant GPCRs inhibitory potencies with IC_{50} values of 0.15, 0.02, and 0.76 nM, respectively. SARs of coumarin derivatives from inhibitors to activators on GPCRs are shown in Figure 3 on the basis of the data (Table 1). Notably, the acylation of hydroxyl groups at the C-7 and C-8 positions of the 7,8-dihydroxycoumarin skeleton, or the etherification of the hydroxyl group at the C-7 position of the 7-hydroxycoumarin skeleton, can successfully change GPCR activators into inhibitors. This work demonstrates a simple and efficient approach to develop coumarin derivatives into remarkable GPCRs activators and inhibitors via molecular diversity-based synthesis.

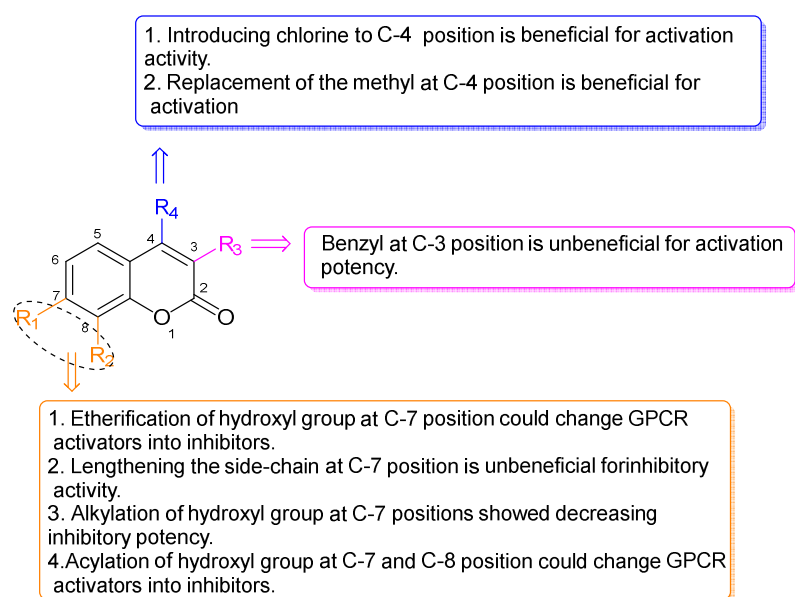


Figure 3. The SARs of coumarin derivatives in GPCR bioactivity.

Supplementary Materials: The following supporting information can be downloaded at: <https://www.mdpi.com/article/10.3390/polym14102021/s1>, Figures S1–S72: The NMR spectra and ESI-MS spectroscopy dates of compounds 1–25; Figures S73–S75: The relationship between concentrate and inhibition rate of compounds 1–25. References [52–59,61] are cited in the supplementary materials.

Author Contributions: R.G. designed the experiment and prepared the manuscript. W.W. and F.W. proposed some instructions for the experiment. L.Z., Z.F., X.S., N.L., Z.W. and S.W. synthesized compounds and collected the experimental data. R.S. and S.H. revised the manuscript. R.G. gave final approval for the version of the manuscript that was submitted. All authors have read and agreed to the published version of the manuscript.

Funding: The work was supported by the National Natural Science Foundation of China (Nos. 81502955 and 82173731), and the Shanghai Frontiers Research Center of the Hadal Biosphere. Ruilong Sheng appreciate FCT-Fundação para a Ciência e a Tecnologia (Base Fund UIDB/00674/2020 and FCT employment fund 2021.00453.CEECIND) and ARDITI-Agência Regional para o Desenvolvimento da Investigação Tecnologia e Inovação through the project M1420-01-0145-FEDER-000005-CQM+(Madeira 14–20 Program), and ARDITI-CQM-2017-ISG-003 for their sponsorship.

Institutional Review Board Statement: Not applicable.

Informed Consent Statement: Not applicable.

Data Availability Statement: The data presented in this study are available on request from the corresponding author.

Acknowledgments: The authors would like to acknowledge the financial support from the National Natural Science Foundation of China, Shanghai Frontiers Research Center of the Hadal Biosphere, FCT-Fundação para a Ciência e a Tecnologia, and ARDITI-Agência Regional para o Desenvolvimento da Investigação Tecnologia e Inovação.

Conflicts of Interest: The authors declare no conflict of interest.

References

1. Katritch, V.; Cherezov, V.; Stevens, R.C. Structure-function of the G protein-coupled receptor superfamily. *Annu. Rev. Pharmacol. Toxicol.* **2013**, *53*, 531–556. [[CrossRef](#)] [[PubMed](#)]
2. Wettschureck, N.; Offermanns, S. Mammalian G proteins and their cell type specific functions. *Physiol. Rev.* **2005**, *85*, 1159–1204. [[CrossRef](#)] [[PubMed](#)]
3. Zhang, H.; Qiao, A.; Yang, D.; Yang, L.; Dai, A.; de Graaf, C.; Reedtz-Runge, S.; Dharmarajan, V.; Zhang, H.; Han, G.W.; et al. Structure of the full-length glucagon class B G-protein-coupled receptor. *Nature* **2017**, *546*, 259–264. [[CrossRef](#)] [[PubMed](#)]
4. Hauser, A.S.; Attwood, M.M.; Rask-Andersen, M.; Schioth, H.B.; Gloriam, D.E. Trends in GPCR drug discovery: New agents, targets and indications. *Nat. Rev. Drug. Discov.* **2017**, *16*, 829–842. [[CrossRef](#)]
5. Sriram, K.; Insel, P.A. G Protein-Coupled receptors as targets for approved drugs: How many targets and how many drugs? *Mol. Pharmacol.* **2018**, *93*, 251–258. [[CrossRef](#)]
6. Yoon, S.C.; Bruner, H.C. Naloxegol in opioid-induced constipation: A new paradigm in the treatment of a common problem, Patient. *Prefer. Adherence* **2017**, *11*, 1265–1271. [[CrossRef](#)]
7. Hauser, R.A.; Hewitt, L.A.; Isaacson, S. Droxidopa in patients with neurogenic orthostatic hypotension associated with Parkinson's disease (NOH306A). *J. Parkinsons. Dis.* **2014**, *4*, 57–65. [[CrossRef](#)]
8. Turncliff, R.; Hard, M.; Du, Y.; Risinger, R.; Ehrich, E.W. Relative bioavailability and safety of aripiprazole lauroxil, a novel once-monthly, long-acting injectable atypical antipsychotic, following deltoid and gluteal administration in adult subjects with schizophrenia. *Schizophr. Res.* **2014**, *159*, 404–410. [[CrossRef](#)]
9. Hope, J.; Castle, D.; Keks, N.A. Brexpiprazole: A new leaf on the partial dopamine agonist branch. *Australas Psychiatry* **2018**, *26*, 92–94. [[CrossRef](#)]
10. Pola, S.; Shah, S.R.; Pingali, H.; Zaware, P.; Thube, B.; Makadia, P.; Patel, H.; Bandyopadhyay, D.; Rath, A.; Giri, S.; et al. Discovery of a potent G-protein-coupled receptor 119 agonist for the treatment of type 2 diabetes. *Bioorg. Med. Chem.* **2021**, *35*, 116071. [[CrossRef](#)]
11. Wang, Y.; Chen, H.; Sheng, R.; Fu, Z.; Fan, J.; Wu, W.H.; Tu, Q.; Guo, R. Synthesis and bioactivities of marine pyran-isoindolone derivatives as potential antithrombotic agents. *Mar. Drugs.* **2021**, *19*, 218. [[CrossRef](#)] [[PubMed](#)]
12. Wang, J.; Lu, S.; Sheng, R.; Fan, J.; Wu, W.; Guo, R. Structure-activity relationships of natural and synthetic indole-derived scaffolds as alpha-glucosidase inhibitors: A mini-review, *Mini. Rev. Med. Chem.* **2020**, *20*, 1791–1818. [[CrossRef](#)] [[PubMed](#)]
13. Bian, C.; Wang, J.; Zhou, X.; Wu, W.; Guo, R. Recent advances on marine alkaloids from sponges. *Chem. Biodivers.* **2020**, *17*, e2000186. [[CrossRef](#)] [[PubMed](#)]
14. Lu, S.; Wang, J.; Sheng, R.; Fang, Y.; Guo, R. Novel bioactive polyketides isolated from marine actinomycetes: An update review from 2013 to 2019. *Chem. Biodivers.* **2020**, *17*, e2000562. [[CrossRef](#)] [[PubMed](#)]
15. Zhang, Y.; Cheng, K.; Xu, B.; Shi, J.; Qiang, J.; Shi, S.; Yi, Y.; Li, H.; Jin, T.; Guo, R.; et al. Epigenetic input dictates the threshold of targeting of the integrin-dependent pathway in non-small cell lung cancer. *Front. Cell. Dev. Biol.* **2020**, *8*, 652. [[CrossRef](#)]
16. Wang, J.; Su, S.; Zhang, S.; Zhai, S.; Sheng, R.; Wu, W.; Guo, R. Structure-activity relationship and synthetic methodologies of alpha-santonin derivatives with diverse bioactivities: A mini-review. *Eur. J. Med. Chem.* **2019**, *175*, 215–233. [[CrossRef](#)]
17. Guo, R.; Duan, D.; Hong, S.; Zhou, Y.; Wang, F.; Wang, S.; Wu, W.; Bao, B. A marine fibrinolytic compound FGFC1 stimulating enzymatic kinetic parameters of a reciprocal activation system based on a single chain urokinase-type plasminogen activator and plasminogen. *Process. Biochem.* **2018**, *68*, 190–196. [[CrossRef](#)]
18. Guo, R.; Guo, C.; He, D.; Zhao, D.; Shen, Y. Two new C19-diterpenoid alkaloids with anti-inflammatory activity from *Aconitum iochanicum*. *Chin. J. Chem.* **2017**, *35*, 1644–1647. [[CrossRef](#)]
19. Guo, R.; Zhang, Y.; Duan, D.; Fu, Q.; Zhang, X.; Yu, X.; Wang, S.; Bao, B.; Wu, W. Fibrinolytic evaluation of compounds isolated from a marine fungus *stachybotrys longispora* FG216. *Chin. J. Chem.* **2016**, *34*, 1194–1198. [[CrossRef](#)]
20. Wang, G.; Wu, W.; Zhu, Q.; Fu, S.; Wang, X.; Hong, S.; Guo, R.; Bao, B. Identification and fibrinolytic evaluation of an isoindolone derivative isolated from a rare marine fungus *Stachybotrys longispora* FG216. *Chin. J. Chem.* **2015**, *33*, 1089–1095. [[CrossRef](#)]
21. Li, J.; Yang, X.M.; Jiang, W.; Hu, Q.Q.; Wang, X.J.; Xu, H.H. Recent Advances on Anticancer Effects and Molecular Mechanisms of Maslinic Acid. *Med. Res.* **2022**, *6*, 220002.
22. Wang, X.W.; Yang, Y.Q.; Li, Y.; Ba, C.F. Acteoside Attenuates Retinal Ganglion Cell Damage in Acute High Intraocular Pressure-Induced Rats via the Bax/Bcl-xL Axis. *Med. Res.* **2022**, *6*, 220001.
23. Wang, H.; Dong, H.Y.; Liu, Y.F.; Ma, Y.X.; Wang, W.; Guo, Z.M.; Wang, C.R. Chemical Research on Limonoids Isolated from the Fruits of *Melia toosendan*. *Med. Res.* **2022**, *6*, 210014.
24. Zheng, S.D.; Fang, H.; Liu, J.F. Study on Chemical Constituents and Bioactivities from *Eucalyptus globulus*. *Med. Res.* **2021**, *5*, 210007.

25. Fang, H.; Zheng, S.D.; Liu, J.F. Progress in Chemical Constituents and Bioactivities of *Perilla frutescens* (L.). *Britt. Med. Res.* **2021**, *5*, 210008.
26. Molnar, M.; Lončarić, M.; Kovač, M. Green chemistry approaches to the synthesis of coumarin derivatives. *Curr. Org. Chem.* **2020**, *24*, 4–43. [[CrossRef](#)]
27. Bourgaud, F.; Poutaraud, A.; Guckert, A. Extraction of coumarins from plant material (Leguminosae). *Phytochem. Anal.* **1994**, *5*, 127–132. [[CrossRef](#)]
28. Qu, D.; Hou, Z.; Li, J.; Luo, L.; Su, S.; Ye, Z.; Bai, Y.; Zhang, X.; Chen, G.; Li, Z.; et al. A new coumarin compound DCH combats methicillin-resistant *Staphylococcus aureus* biofilm by targeting arginine repressor. *Sci. Adv.* **2020**, *6*, 9597–9611. [[CrossRef](#)]
29. Mangasuli, S.N.; Hosamani, K.M.; Devarajegowda, H.C.; Kurjogi, M.M.; Joshi, S.D. Synthesis of coumarin-theophylline hybrids as a new class of anti-tubercular and anti-microbial agents. *Eur. J. Med. Chem.* **2018**, *146*, 747–756. [[CrossRef](#)]
30. Salvador, J.P.; Tassies, D.; Reverter, J.C.; Marco, M.P. Enzyme-linked immunosorbent assays for therapeutic drug monitoring coumarin oral anticoagulants in plasma. *Anal. Chim. Acta.* **2018**, *1028*, 59–65. [[CrossRef](#)]
31. Emam, S.H.; Sonousi, A.; Osman, E.O.; Hwang, D.; Kim, G.D.; Hassan, R.A. Design and synthesis of methoxyphenyl- and coumarin-based chalcone derivatives as anti-inflammatory agents by inhibition of NO production and down-regulation of NF-kappaB in LPS-induced RAW264.7 macrophage cells. *Bioorg. Chem.* **2021**, *107*, 104630. [[CrossRef](#)] [[PubMed](#)]
32. Zhao, Y.L.; Yang, X.W.; Wu, B.F.; Shang, J.H.; Liu, Y.P.; Zhi, D.; Luo, X.D. Anti-inflammatory effect of Pomelo Peel and its bioactive coumarins. *J. Agric. Food. Chem.* **2019**, *67*, 8810–8818. [[CrossRef](#)] [[PubMed](#)]
33. Zhu, Z.; Su, Z.; Yang, J.; Liu, H.; Tang, M.; Hu, Q.; Bai, P.; Wen, J.; He, J.; Niu, T.; et al. Anti-tumor study of H6, a 4-substituted coumarins derivative, loaded biodegradable self-assembly nano-micelles in vitro and in vivo. *J. Biomed. Nanotechnol.* **2019**, *15*, 1515–1531. [[CrossRef](#)] [[PubMed](#)]
34. Wu, Y.; Xu, J.; Liu, Y.; Zeng, Y.; Wu, G. A review on anti-tumor mechanisms of coumarins. *Front. Oncol.* **2020**, *10*, 592853. [[CrossRef](#)] [[PubMed](#)]
35. Shahzadi, I.; Ali, Z.; Baek, S.H.; Mirza, B.; Ahn, K.S. Assessment of the antitumor potential of umbelliprenin, a naturally occurring sesquiterpene coumarin. *Biomedicines* **2020**, *8*, 126. [[CrossRef](#)]
36. Wang, G.; Liu, Y.; Zhang, L.; An, L.; Chen, R.; Liu, Y.; Luo, Q.; Li, Y.; Wang, H.; Xue, Y. Computational study on the antioxidant property of coumarin-fused coumarins. *Food. Chem.* **2020**, *304*, 125446. [[CrossRef](#)]
37. Safakish, M.; Hajimahdi, Z.; Aghasadeghi, M.R.; Vahabpour, R.; Zarghi, A. Design, synthesis, molecular modeling and anti-HIV assay of novel quinazolinone Incorporated coumarin derivatives. *Curr. HIV Res.* **2020**, *18*, 41–51. [[CrossRef](#)]
38. Gao, Y.; Cheng, H.; Khan, S.; Xiao, G.; Rong, L.; Bai, C. Development of coumarine derivatives as potent anti-filovirus entry inhibitors targeting viral glycoprotein. *Eur. J. Med. Chem.* **2020**, *204*, 112595. [[CrossRef](#)]
39. Hu, Y.H.; Yang, J.; Zhang, Y.; Liu, K.C.; Liu, T.; Sun, J.; Wang, X.J. Synthesis and biological evaluation of 3-(4-aminophenyl)-coumarin derivatives as potential anti-alzheimer's disease agents. *J. Enzyme. Inhib. Med. Chem.* **2019**, *34*, 1083–1092. [[CrossRef](#)]
40. Annunziata, F.; Pinna, C.; Dallavalle, S.; Tamborini, L.; Pinto, A. An overview of coumarin as a versatile and readily accessible scaffold with broad-ranging biological activities. *Int. J. Mol. Sci.* **2020**, *21*, 4618. [[CrossRef](#)]
41. Loncaric, M.; Strelec, I.; Pavic, V.; Subaric, D.; Rastija, V.; Molnar, M. Lipoygenase inhibition activity of coumarin derivatives-QSAR and molecular docking study. *Pharmaceuticals* **2020**, *13*, 154. [[CrossRef](#)]
42. Tian, D.; Wang, F.; Duan, M.; Cao, L.; Zhang, Y.; Yao, X.; Tang, J. Coumarin analogues from the citrus grandis (L.) osbeck and their hepatoprotective activity. *J. Agric. Food. Chem.* **2019**, *67*, 1937–1947. [[CrossRef](#)] [[PubMed](#)]
43. Potdar, M.K.; Mohile, S.S.; Salunkhe, M.M. Coumarin syntheses via pechmann condensation in lewis acidic chloroaluminate ionic liquid. *Cheminform* **2002**, *42*, 9285–9287. [[CrossRef](#)]
44. Rosen, T. The perkin reaction. In *Comprehensive Organic Synthesis*; Trost, B.M., Fleming, I., Eds.; Sciencedirect: Amsterdam, The Netherlands, 1991; Volume 2, pp. 395–408.
45. Watson, B.T.; Christiansen, G.E. Solid phase synthesis of substituted coumarin-3-carboxylic acids via the Knoevenagel condensation. *Tetrahedron. Lett.* **1998**, *39*, 6087–6090. [[CrossRef](#)]
46. Jadhav, N.H.; Sakate, S.S.; Rasal, N.K.; Shinde, D.R.; Pawar, R.A. Heterogeneously catalyzed pechmann condensation employing the tailored Zn_{0.925}Ti_{0.075}O NPs: Synthesis of coumarin. *ACS. Omega* **2019**, *4*, 8522–8527. [[CrossRef](#)] [[PubMed](#)]
47. Ouellette, R.J.; Rawn, J.D. *Aldehydes and Ketones: Nucleophilic Addition Reactions*; Sciencedirect: Amsterdam, The Netherlands, 2018; pp. 595–623.
48. Laufer, M. Synthesis of 7-hydroxycoumarins by Pechmann reaction using Nafion resin/silica nanocomposites as catalysts. *J. Catal.* **2003**, *218*, 315–320. [[CrossRef](#)]
49. Ryabukhin, D.S.; Vasilyev, A.V. Synthesis of (iso)quinoline, (iso)coumarin and (iso)chromene derivatives from acetylene compounds. *Russ. Chem. Rev.* **2016**, *85*, 637–665. [[CrossRef](#)]
50. Wang, Y.; Wang, J.; Fu, Z.; Sheng, R.; Wu, W.; Fan, J.; Guo, R. Syntheses and evaluation of daphnetin derivatives as novel G protein-coupled receptor inhibitors and activators. *Bioorg. Chem.* **2020**, *104*, 104342. [[CrossRef](#)]
51. Graaf, C.D.; Song, G.; Cao, C.; Zhao, Q.; Wang, M.W.; Wu, B.; Stevens, R.C. Extending the Structural View of Class B GPCRs. *Trends Biochem. Sci.* **2017**, *42*, 946–960. [[CrossRef](#)]
52. Katkevi, S.M.; Kontijevskis, A.; Mutule, I. Microwave-Promoted Automated Synthesis of a Coumarin Library. *Chem. Heterocycl. Compd.* **2007**, *43*, 151–159. [[CrossRef](#)]

53. Tiftikçi, E.; Erk, Ç. The synthesis of novel crown ethers, Part X—4-propyl- and 3-ethyl-4-methylchromenone-crown ethers. *J. Heterocyclic Chem.* **2010**, *41*, 867–871. [[CrossRef](#)]
54. Madhav, J.V.; Kuarm, B.S.; Someshwar, P. ChemInform Abstract: Dipyrindine Cobalt Chloride: A Novel Catalyst for the Synthesis of Coumarins via Pechmann Condensation. *J. Chem. Res.* **2010**, *2008*, 867–871. [[CrossRef](#)]
55. Lu, Z.L.; Neverov, A.A.; Brown, R.S. An ortho-palladated dimethylbenzylamine complex as a highly efficient turnover catalyst for the decomposition of P=S insecticides. Mechanistic studies of the methanolysis of some P=S-containing phosphorothioate triesters. *Org. Biomol. Chem.* **2005**, *3*, 3379–3387. [[CrossRef](#)]
56. Qing, S.; Quan, P.; Jialiang, S.; Xuefeng, L. Synthesis and biological evaluation of functionalized coumarins as acetylcholinesterase inhibitors. *Eur. J. Med. Chem.* **2005**, *40*, 1307–1315.
57. Fall, Y.; Santana, L.; Uriarte, E. Synthesis and characterization of some coumarins with two hydroxy or methoxy substituents. *J. Heterocyclic Chem.* **2001**, *38*, 1231–1232. [[CrossRef](#)]
58. Timonen, J.M.; Nieminen, R.M.; Sareila, O. Synthesis and anti-inflammatory effects of a series of novel 7-hydroxycoumarin derivatives. *Eur. J. Med. Chem.* **2011**, *46*, 3845–3850. [[CrossRef](#)] [[PubMed](#)]
59. Pisani, L.; Muncipinto, G.; Miscioscia, T.F.; Nicolloti, O.; Leonetti, F.; Catto, M.; Caccia, C.; Salvati, P.; Soto-Otero, R.; Mendez-Alvarez, E.; et al. Discovery of a Novel Class of Potent Coumarin Monoamine Oxidase B Inhibitors: Development and Biopharmacological Profiling of 7-[(3-Chlorobenzyl)oxy]-4-[(methylamino)methyl]-2H-chromen-2-one Methanesulfonate (NW-1772) as a Highly Potent, Selective, Reversible, and Orally Active Monoamine Oxidase B Inhibitor. *J. Med. Chem.* **2009**, *52*, 6685–6706.
60. Sun, W.; Hu, S.; Fang, S.; Yan, H. Design, synthesis and biological evaluation of pyrimidine-based derivatives as VEGFR-2 tyrosine kinase inhibitors. *Bioorg. Chem.* **2018**, *78*, 393–405. [[CrossRef](#)]
61. Kim, S.; Kang, D.; Lee, C.H. ChemInform Abstract: Synthesis of Substituted Coumarins via Broensted Acid Mediated Condensation of Allenes with Substituted Phenols or Anisoles. *J. Org. Chem.* **2012**, *77*, 6530–6537. [[CrossRef](#)]
62. Wang, J.; Bian, C.; Wang, Y.; Shen, Q.; Bao, B.; Fan, J.; Zuo, A.; Wu, W.; Guo, R. Syntheses and bioactivities of songorine derivatives as novel G protein-coupled receptor antagonists. *Bioorg. Med. Chem.* **2019**, *27*, 1903–1910. [[CrossRef](#)]
63. Zhuang, Y.; Xu, G.; Zhang, L.; Zha, J.K.; Ji, P.P.; Li, Y.N.; Liu, B.Y.; Zhang, J.F.; Zhao, Q.; Sun, Y.N.; et al. Development of a double monoclonal antibody-based sandwich enzyme-linked immunosorbent assay for detecting canine distemper virus. *Appl. Microbiol. Biot.* **2020**, *104*, 10725–10735. [[CrossRef](#)] [[PubMed](#)]
64. Kimman, T.G.; Leeuw, D.O.; Kochan, G.; Szewczyk, B.; Rooij, V.E.; Jacobs, L.; Kramps, J.; Peeters, V. An indirect double-antibody sandwich enzyme-linked immunosorbent assay (ELISA) using baculovirus-expressed antigen for the detection of antibodies to glycoprotein E of pseudorabies virus and comparison of the method with blocking ELISAs. *Clin. Diagn. Lab. Immun.* **1996**, *3*, 167–174. [[CrossRef](#)] [[PubMed](#)]
65. Jung, K.; Park, Y.J.; Ryu, J.S. Scandium(III) triflate-catalyzed coumarin synthesis. *Synth. Commun.* **2008**, *38*, 4395–4406. [[CrossRef](#)]
66. Xiao, F.L. *The Study of General Toxicology for a New Anticoccidial Triazine Grug Ethanamizuril*; Chinese Academy of Agricultural Sciences: Beijing, China, 2014.